PWA/Silica Doped Sulfonated Poly(ether sulfone) Composite Membranes for Direct Methanol Fuel Cells

Chien-Chung Chen,[1] Hung-Yi Tsi,[2] Wen-Chin Tsen,[2] Fu-Sheng Chuang,[2] Shin-Cheng Jang,[3] Yao-Chi Shu,[2] Sheng Wen,[4] Chunli Gong[4]

[1]*Graduate Institute of Biomedical Materials and Engineering, Department of Oral Medicine, Taipei Medical University, Taipei, Taiwan, Republic of China*
[2]*Department of Polymer Materials, Vanung University, Tao-Yuan 32045, Taiwan, Republic of China*
[3]*Department of Fashion Design, Ling Tung University, Taichung, Taiwan Republic of China*
[4]*Department of Chemistry and Material Science, Xiaogan University, Xiaogan, Hubei 432100, China*

Received 15 May 2010; accepted 29 March 2011
DOI 10.1002/app.34602
Published online 12 August 2011 in Wiley Online Library (wileyonlinelibrary.com).

ABSTRACT: A novel sulfonated poly(ether sulfone) (SPES)/phosphotungstic acid (PWA)/silica composite membranes for direct methanol fuel cells (DMFCs) application were prepared. The structure and performance of the obtained membranes were characterized by thermogravimetric analysis (TGA), differential scanning calorimetry (DSC), scanning electron microscopy (SEM), water uptake, proton conductivity, and methanol permeability. Compared to a pure SPES membrane, PWA and SiO_2 doped membranes had a higher thermal stability and glass transition temperature (T_g) as revealed by TGA-FTIR and DSC. The morphology of the composite membranes indicated that SiO_2 and PWA were uniformly distributed throughout the SPES matrix. Proper PWA and silica loadings in the composite membranes showed high proton conductivity and sufficient methanol permeability. The selectivity (the ratio of proton conductivity to methanol permeability) of the SPES-P-S 15% composite membrane was almost five times than that of Nafion 112 membrane. This excellent selectivity of SPES/PWA/silica composite membranes indicate a potential feasibility as a promising electrolyte for DMFC.
 J Appl Polym Sci 123: 1184–1192, 2012

Key words: sulfonated poly(ether sulfones); phosphotungstic acid; composite membrane; direct methanol fuel cells

INTRODUCTION

Fuel cells have been identified as a very feasible energy source with minimal noxious emissions and have been the subject of academic and industrial interest for over a decade.[1] Among the various fuel cells, direct methanol fuel cells (DMFCs) are the most suitable for portable devices (cell phones and laptops), because they have a high charge density, low operating temperature, and simple fuel-cell setup (with easy storage of methanol and no need for a reformer).[2–4] The electrolyte is the most important component in any fuel-cell system. One of the main components in DMFCs is the electrolyte membrane. Dupont Nafion® or other perfluorinated sulfonic acid membranes are widely acknowledged good electrolyte membranes, because of their high proton conductivity and chemical stability. However, the perfluorinated sulfonic acid membranes used in DMFCs are expensive and have relatively poor resistance to methanol transport.[5]

Great efforts have been dedicated to develop membrane materials with high proton conductivity and low methanol permeability. The addition of inorganic materials into a sulfonated polymer matrix has attracted more and more interests. Up to now, many people have reported the properties of sulfonated polymer/silica-based composites. Jiang et al.[6] and Mauritz and Payne[7] prepared silica/Nafion composite membranes by sol-gel reaction and used them in DMFCs. They found that the silica doped in the membranes could obviously slow the methanol permeation. Tsai et al.[8] prepared the nanocomposite membranes by incorporating silica into sulfonated 4,4′-dihydroxy-α-methylstilbene (HMS)-based poly(arylene ether sulfone) copolymer. The membrane showed higher single cell performance compared to the Nafion® 117 membrane in DMFCs at 80°C. Lee et al.[9] prepared a similar type of composite membrane in DMFCs and investigated the influence of SiO_2 nanoparticles with different surface properties on the properties of composite membranes. It was found that SiO_2 could hold up methanol transport and increase water uptake of membranes especially at high temperature. However, when the SiO_2

Correspondence to: Yao-Chi Shu (ycs1226@mail.vnu.edu.tw).
Contract grant sponsor: Hubei Provincial Department of Education.

doping content exceeded a specific range, the proton conductivity dropped significantly due to the nonconductive of the hygroscopic oxides themselves.[10] The similar phenomenon was detected in sulfonated polyether sulfone (SPES)/SiO_2 composite membranes, as described in our previous work.[11]

Heteropolyacid (HPA), such as phosphotungstic acid (PWA), is one of the attractive inorganic additives because of their high proton conductivity and thermal stability in crystalline form.[12,13] Fenton and coworkers[14] recast the Nafion/HPA composite for H_2/O_2 fuel cell and found that the HPA could increase the conductivity of the membrane. Staiti et al.[15] and Shao et al.[16] evaluated PWA-doped composite silica/Nafion/PWA membranes for high-temperature DMFCs (145°C). Kim et al. studied the composite membranes of PWA and sulfonated poly(arylene ether sulfone), achieving a proton conductivity of 0.15 S cm^{-1}.[17] In this work, we try to maintain low methanol permeability and high proton conductivity with the incorporation of silica and PWA. The SPES/PWA/SiO_2 composite membranes with various PWA and silica loadings were prepared by doping SiO_2 sol and PWA in the SPES matrix. The morphologies and properties, including the thermal and water uptake, proton conductivities, and methanol permeability, have been varied by the variation of the composition of the composite membrane.

EXPERIMENTAL

Sulfonation of PES

Sulfonation of PES (Ultrason® E6020P, T_g = 225°C, M_w = 51 kg mol^{-1}, M_w/M_n = 3.5, BASF) was carried out in concentrated sulfuric acid (98%) solvent using chlorosulfonic acid as a sulfonating agent as described by Dai et al.[18] The degree of sulfonation (DS) of the obtained SPES was 35%, that is, the ion exchange capacity (IEC) value was 1.34 meq g^{-1}.

Preparation of composite membranes

SPES was dissolved in DMAc to form a 10 wt % transparent solution, PWA was dissolved in deionized water, and then the TEOS was added at a 2 : 5 weight ratio of PWA to SiO_2. The PWA and TEOS solutions were shortly mixed the SPES solution. The formed solution was magnetically stirred for 1 h and degassed by ultrasonication. The content of SiO_2 in the mixture were varied in 5, 10, 15, and 20 wt % based on SPES. To remove any impurity, the solutions were filtered through a 0.2 mm pore size Teflon filter before membrane casting. The prepared mixture was slowly poured into a glass dish in an amount that would give a thickness of $\sim$ 60 μm of the formed composite membrane. The produced membranes were dried at 80°C for 4 h, followed by 120°C for another 12 h in air, and then vacuum-dried at 120°C for 24 h. Hereafter, the notations of composite membranes are denoted as SPES-P-S x, where x is the weight percentage of SiO_2 in the SPES matrix.

Thermogravimetric analysis (TGA)-FTIR

The thermogravimetric spectra were obtained by TGA (TA SDT-Q600). The samples were initially heated up to 220°C for 30 min to remove the absorbed water, then cooled down to 50°C and reheated to 800°C at a heating rate of 10°C min^{-1} in nitrogen. The TGA outlet was coupled on-line with a Nicolet 380 FTIR spectrometer through a gas cell, which was warmed up to 240°C and stabilized for 2 h before performing TGA.

Differential scanning calorimetry (DSC)

The glass transition temperatures (T_g) were obtained with a Perkin–Elmer DSC-7 under nitrogen at a heating rate of 10°C min^{-1}. Scans were conducted by heating up to 220°C, and annealed for 10 min to eliminate the prior thermal and solvent histories, followed by quenching quickly to room temperature. The T_g value was reported as the midpoint of the change in the slope of the baseline.

Morphology

The cross section of the membranes was examined with a scanning electron microscope (SEM) (HITACHI X-650) equipped with an energy dispersive X-ray spectrometer. The membranes were fractured by brief immersion in liquid nitrogen. Fresh cross section cryogenic fractures of the membranes were vacuum-sputtered with a thin layer of Pt/Pd prior to analysis.

Water uptake

The composite membranes were dried in a vacuum oven at 100°C for 24 h, weighed (W_{dry}), and immersed in deionized water at different temperature for 48 h. Then, the wet membranes were blotted to remove surface water droplets and quickly weighed (W_{wet}). The water uptake of membranes was calculated as follows:

$$\text{Water uptake } (\%) = \frac{W_{wet} - W_{dry}}{W_{dry}} \times 100\%. \quad (1)$$

PWA extraction

The amount of PWA extracted from the composite membranes was determined by weight loss. The membranes were first dried in a vacuum oven at

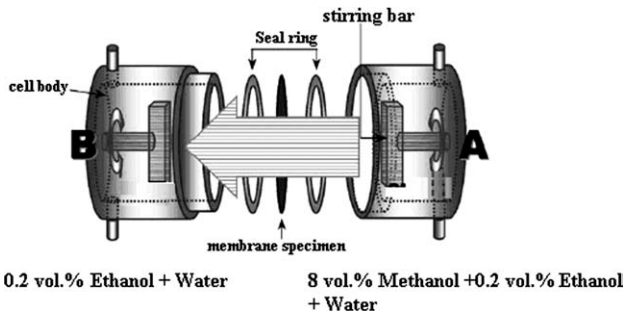

Figure 1 Experimental setup of measurement for methanol permeability.

100°C for 24 h. After drying, the membranes were weighed to obtain an initial weight. They were then immersed in deionized water at room temperature for 24 h, followed by immersing in boiling water for another 24 h. The membranes were finally dried in a vacuum oven at 100°C for 24 h and weighed again. The PWA extraction values were recorded as a weight loss percentage.

Proton conductivity

Proton conductivties of composite membranes were measured with the AC impedance method. In a chamber, the tested membranes (3 × 3 cm) were put into the clamp, which is connected to a complex impedance analyzer (Solatron 1260 Impedance Analyzer) through two platinum electrodes. The frequency range was varied from 0.1 Hz to 10 MHz and the AC voltage amplitude was fixed at 10 mV. All membranes were hydrated by immersing in deionized water for 24 h at room temperature before measuring. The proton conductivity was calculated as follows[19,20]:

$$\sigma = l/Rdw, \tag{2}$$

where, l is the distance between the electrodes; d and w are the thickness and width of the films, respectively, and R is the measured resistance value.

Methanol permeability

Methanol permeability of the membrane was carried out using a two-compartment cell at room temperature as described in our previous work[5,11] and shown in Figure 1.

Initially, the B compartment of the cell (V_B = 20 mL) was filled with a 0.2 vol % ethanol solution in deionized water and the compartment A (V_A = 20 mL) was filled with 8 vol % methanol and 0.2 vol % ethanol and deionized water. The membrane with a diffusion area of 3.14 cm^2, sandwiched by O-ring shape Teflon, was clamped between the two compartments. The membrane samples were equilibrated in deionized water for 24 h before testing. The diffusion cell was kept stirring slowly during experiment. The solution samples (about 2 μL) in compartment B were taken at interval and analyzed by gas chromatography (GC-5890 seriesII, Hewlett–Packard), which is equipped with a HP-20M (CARBOWAX 20M phase) chromatographic column together and a flame ionization detector. Methanol permeability was calculated by following equation:

$$C_B = \frac{D \times K \times C_A \times A}{V_B \times L} \times t, \tag{3}$$

where, C_B is the methanol concentration in compartment B, C_A is the methanol concentration in compartment A, A, L, and V_B are the membrane diffusion area, the thickness and the solution volume of compartment B. D, K, and t are the methanol diffusivity, the solubility and the permeability time, respectively. The methanol permeability (P_m) is defined as the product of diffusivity and solubility (DK).

RESULTS AND DISCUSSION

Thermal stability

TGA-FTIR is an established technique for studying thermal degradation. The representative TG and DTG curves are shown in Figures 2 and 3. Figure 4 presents the stacked FTIR spectra of gas escaping from the composite membrane at various temperatures.

The TGA curve of PWA shows a slight weight loss at about 150°C, probably because of dehydration of the water in crystallization, and then no further significant weight loss is observed until 700°C. As shown in TGA and DTG curves, all the composite

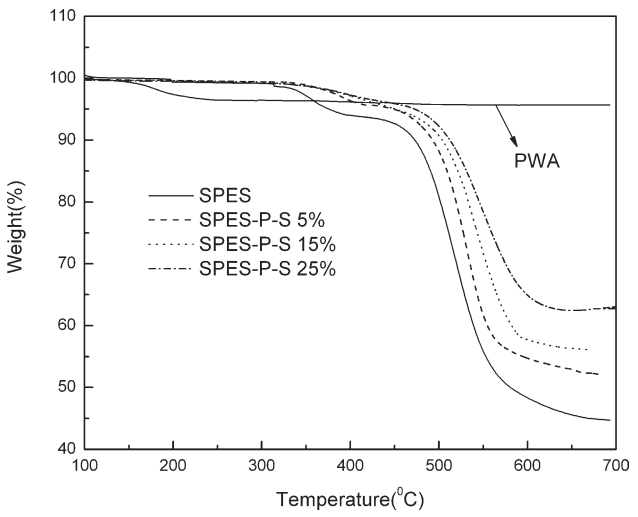

Figure 2 Thermograms of PWA, SPES and composite membranes

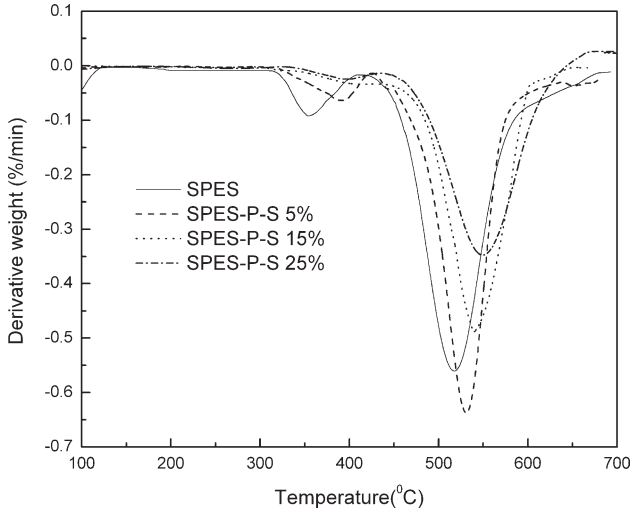

Figure 3 DTG curves of SPES and composite membranes.

membranes exhibited similar two-step degradation pattern. The first shoulder weight loss, starting from −330°C, is believed to be primarily associated with the loss of the sulfonic groups. This fact was evidenced by the FTIR spectra of the gaseous products of the SPES-P-S 15% composite membrane at 400°C. As compared with the first weight loss temperature range, a new peak island appears at around 1365 cm^{-1}, indicating the existence of S=O segments among the gases detected by IR probe. However, the other groups in the PES backbone were not detected in the gaseous products from the second weight loss. Furthermore, the degradation temperature of PES is ~ 500°C, as reported by Guan et al.[21] Therefore, the S=O stretching vibrations at this temperature range should correspond to the evolution of sulfonic acid side groups. Nevertheless, the degradation temperature of sulfonated groups shifted slightly to lower temperatures as the PWA and silica loadings increased. The acid catalysis of PWA should be accounted for the degradation of sulfonated groups.

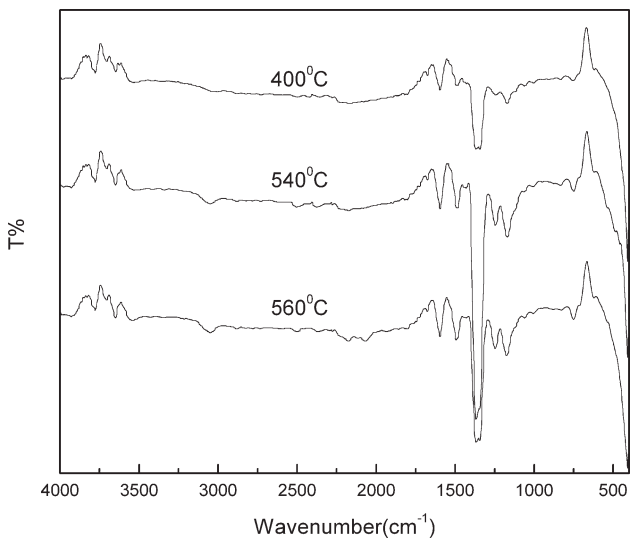

Figure 4 FTIR spectra of gas escaping from the SPES-P-S 15% composite membrane at different temperature.

TABLE I
The Result of Thermal Stabilities

Samples	T_1(°C)[a]	T_2(°C)[b]	T_g(°C)
SPES	315	517	210
SPES-P-S 5%	319	526	215
SPES-P-S 10%	327	536	223
SPES-P-S 15%	335	545	229
SPES-P-S 20%	333	546	231
SPES-P-S 25%	336	550	234

[a] The initial loss temperature of the second stage.
[b] The fastest loss temperature of the third stage.

The second stage occurring at around 470°C is related to the splitting of the polymer main chains. As shown in the FTIR spectra at 540 and 560°C, the peak island at 3060 cm^{-1} (above 3000 cm^{-1}) is the stretching vibration of unsaturated carbon hydrogen bonds, which belong to the phenyl groups. The O=S=O (from 1365 cm^{-1}) can also verifies this result.

As listed in Table I, although the composite membranes showed slightly lower degradation temperature of $-SO_3H$, the significantly higher thermal stabilities of the polymer main chains were observed when compared to the pure SPES membrane, indicating their suitability for high temperature PEMFC.

Glass transition temperature (T_g)

The T_gs of SPES and composite membranes are shown in Figure 5. It can be seen that the T_g of membranes increases with the PWA and silica loadings. For instance, the T_g for SPES was determined to be around 210°C, whereas for SPES-P-W 5%, SPES-P-W 10%, SPES-P-W 15%, and SPES-P-W 25% composite membranes, the temperatures shifted to about 215, 223, 229, and 234°C, respectively. The increment in T_g is attributed to the specific interactions among the sulfonic acid groups in polymer chains, PWA and silica. This result implied that the composite membranes were thermomechanically more stable than the pure SPES membrane.

Morphology

The properties of the membranes were closely related to their microstructures especially the spatial distribution of ionic site and the inorganic particles. Morphological features of the membranes were observed with SEM. The membrane samples were fractured in liquid nitrogen and the fractured cross sections were observed on SEM. The SEM images of

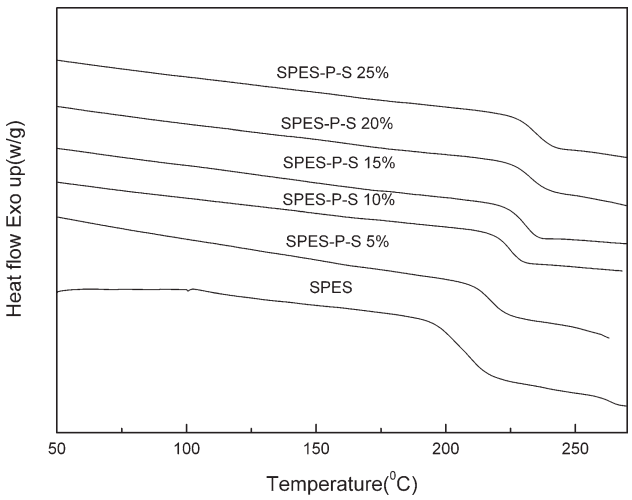

Figure 5 DSC curves of SPES and composite membranes.

SPES-P-S composite membranes at lower and higher magnification are shown in Figures 6 and 7, respectively. For comparison, the SPES/SiO_2 5 and 15% composite membranes were also listed in Figure 7. As shown in Figure 7(a), the SPES membrane shows a very homogeneous and dense cross section. With PWA and SiO_2 content increasing, the spherical silica particles begin to appear in the membranes. The domain size of the inorganic phase increases with the weight ratio of the SiO_2. It is interesting that the silica particles are hardly visible in the SPES-P-S 5% [Fig. 6(b)] membrane, while the SiO_2 particles are clearly observed in the SPES/SiO_2 5% composite membrane. The same tendency is detected in the SPES-P-S 15% and SPES/SiO_2 15% composite membranes. As shown in Figure 6 (c,e), the SPES-P-S 15% composite membrane has smaller particle size and lower particle distribution than that of the SPES/SiO_2 15% composite membranes at the same SiO_2 content. The reason possibly is the hydrolyzation and condensation reactions catalyzed by PWA tighten the microstructure of the membrane and further increase the compatibility of this system.

Water uptake

Water uptake is closely related to the basic membrane properties and plays an essential role in the membrane behavior. Proton conductivity and methanol permeation across the membrane depend to a large extent on the amount and behavior of absorbed

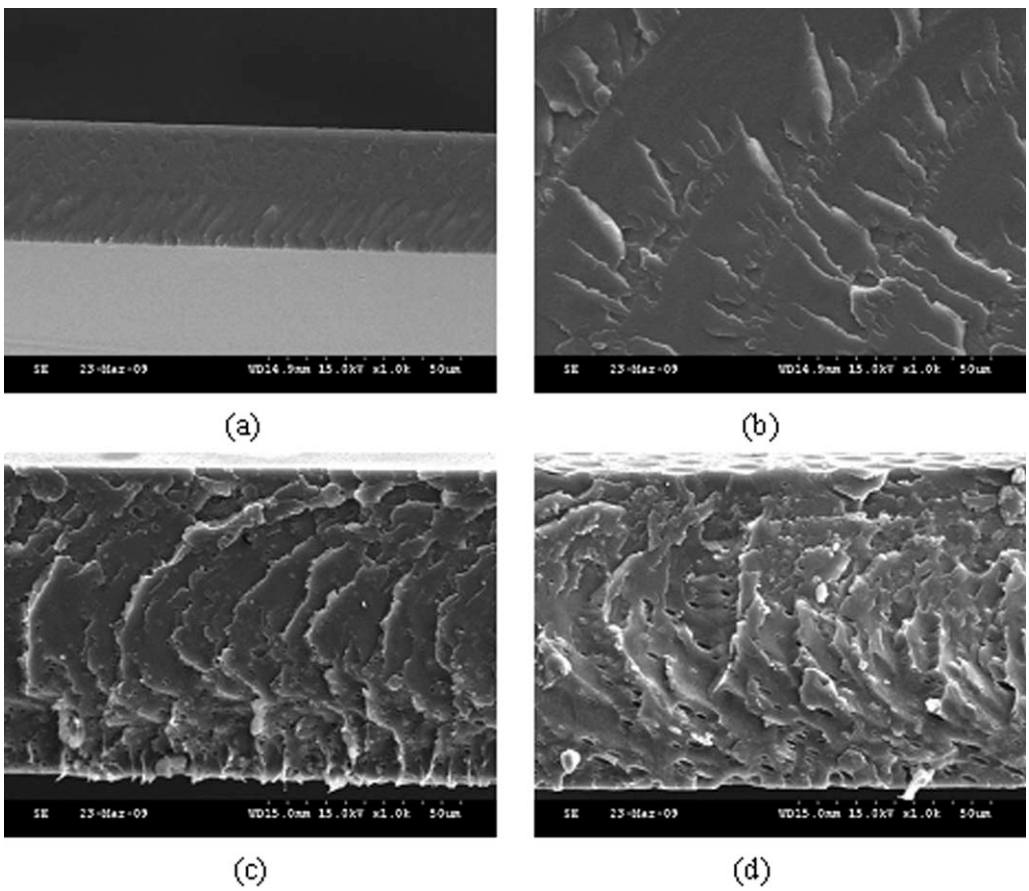

Figure 6 Cross-sectional SEM micrographs of composite membranes at low magnification: (a) SPES; (b) SPES-P-S 5%; (c) SPES-P-S 15%; (d) SPES-P-S 25%.

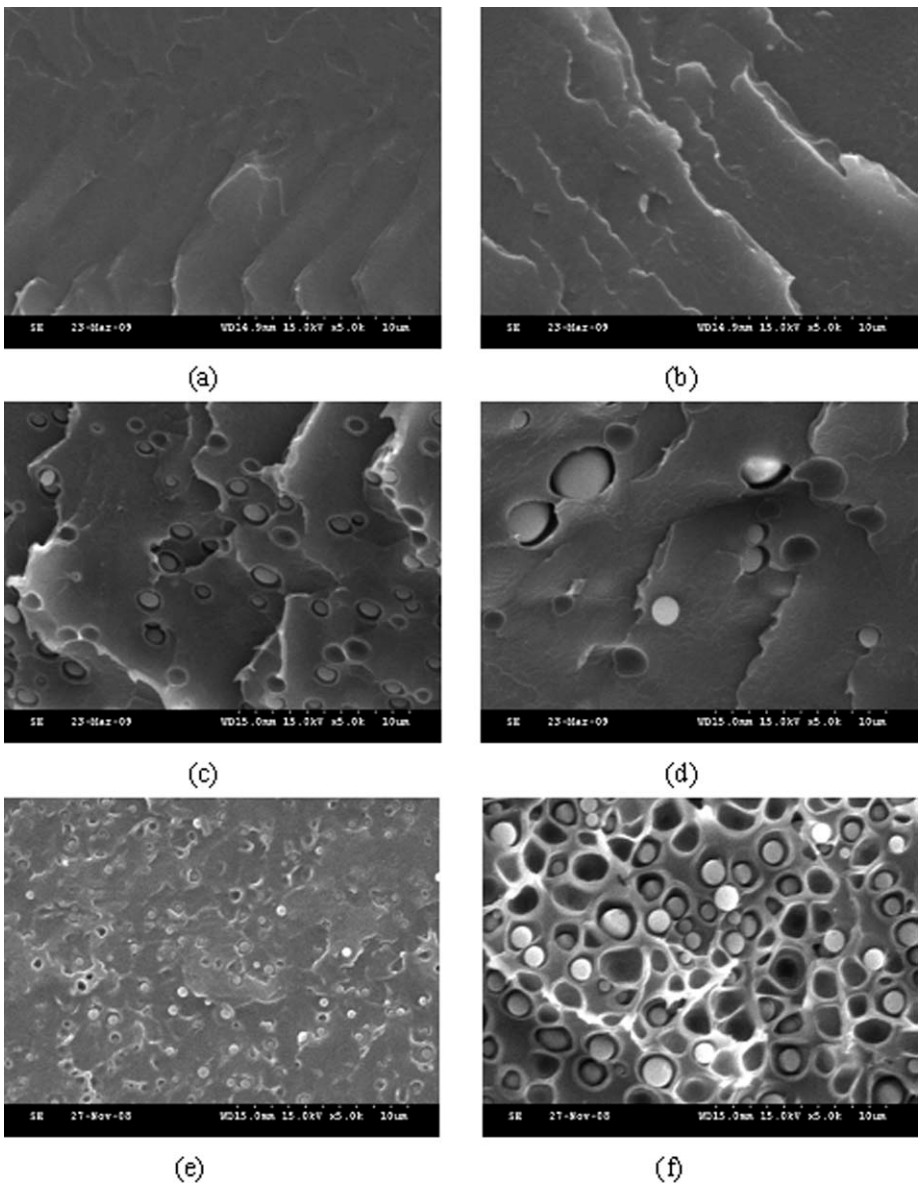

Figure 7 Cross-sectional SEM micrographs of composite membranes at high magnification: (a) SPES; (b) SPES-P-S 5%; (c) SPES-P-S 15%; (d) SPES-P-S 25%; (e) SPES/SiO2 5%; (f) SPES/SiO2 15%.

water in the membrane. Water influences the ionomer microstructure, cluster, and channel size, consequently plasticizers and modifies the mechanical properties. Figure 8 shows the room temperature water uptake of the composite membranes as a function of SiO_2 content. It can be seen that the water uptakes increase with the loading of PWA and SiO_2. The increase in water uptake can be attributed to the water retention of the incorporated silica, which is due to the hydrogen bonding of H_2O molecules with the SiOH groups. Nevertheless, the increasing trend of water uptake in the SPES-P-S composite membranes is lower than that in SPES/SiO_2 composite membranes, as discussed in our earlier work.[11] This slow trend is possibly because of the decrease in the number of available water absorption sites (i.e.,

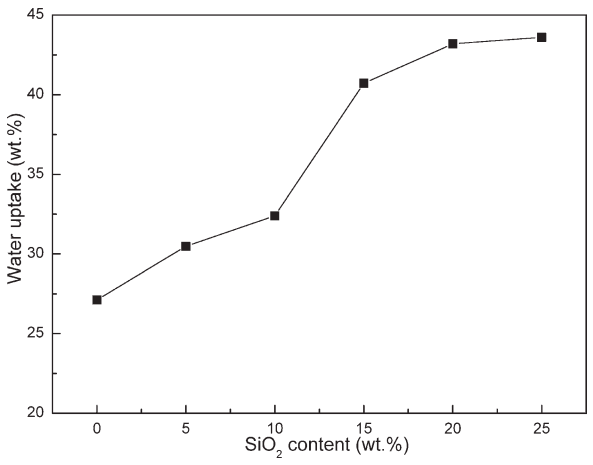

Figure 8 Water uptake of the composite membranes comprised of PWA and silica in varying weight fractions.

TABLE II
PWA Extraction Amount, Proton Conductivity and Methanol Permeability for the Composite Membranes

Samples	Weight loss (%)	Conductivity (S cm^{-1}) 20°C	Conductivity (S cm^{-1}) 80°C	Methanol permeability (cm^2 s^{-1})
SPES	0.0	0.0055	0.011	5.43×10^{-7}
SPES-P-S 5%	0.6	0.008	0.024	4.26×10^{-7}
SPES-P-S 10%	1.5	0.027	0.046	3.08×10^{-7}
SPES-P-S 15%	2.7	0.034	0.069	1.52×10^{-7}
SPES-P-S 20%	3.1	0.023	0.039	1.24×10^{-7}
SPES-P-S 25%	3.7	0.011	0.032	8.38×10^{-8}
Nafion 112	–	0.051	0.075	1.05×10^{-6}

sulfonic acid) resulting from the strong hydrogen bonding interaction between the sulfonic acid and the HPA molecules.[22]

Stability of HPA in the composite membranes

Because the HPA itself is a water soluble material, it would be easily extracted from the composite membrane in the presence of water. This extraction of HPA would lead to a decrease in proton conductivity and durable lifetime in fuel cell systems.[12] Thus the retention of HPA was considered as one of the key parameters on determining the feasibility of the composite membranes used in the fuel cell systems. The extraction values of PWA in SPES/PWA/SiO_2 composite membranes are listed in Table II. The results showed that the extraction of PWA from the composite membranes increased with the PWA content increased. For example, the amount of PWA extraction for SPES-P-S 5% composite membrane was only 0.6%, while the amount of PWA extraction for SPES-P-S 25% composite membrane increased to 3.7%. However, they all showed a negligible PWA extraction. This indicated that the PWA molecules in the membranes were very stable and would not lead out easily. This confirmed the phenomena observed by Xu et al.[23]. The possible reason is that, in this experiment, PWA molecules entered the membrane through the ways opened by TEOS, which partially dissolved the SPES backbone. After the hydrolyzation and condensation reactions of TEOS catalyzed by the acid of PWA, the product of silica network fix up the PWA molecules tightly.

Proton conductivity

The proton conductivity is a decisive property of fuel cell membranes, as the efficiency of the fuel cell depends on the proton conductivity. In general, proton conductivity directly depends on the water uptake and IEC of the sulfonated polymer.[10] Figure 9 compares the proton conductivity of Nafion 112 and SPES-P-S composite membranes at different temperatures. Obviously, the conductivity of all the membranes increased with increasing temperatures and the relationship of ln[σ(S cm^{-1})] and 1000/T accorded with linear function. According to the discussion by Shen et al.[24], this indicated that the relationship between proton conductivity and temperature satisfied an Arrhenius equation [$\sigma = \sigma_0 \exp(-E_a/RT)$]. The conductive active energy (E_a) were calculated by the slops, which are 8.35, 8.42, 11.84, 12.09, and 12.15 kJ mol^{-1} for Nafion 112, SPES, SPES-P-S 5%, SPES-P-S 15%, and SPES-P-S 25%, respectively. The E_a values of SPES-P-S composite membranes are similar and higher than that of Nafion 112 and SPES membranes. This indicated that the degree of proton conductivity increasing with temperature is more obvious than that of Nafion 112 and SPES membranes.

It can also be seen that proton conductivity increased with increasing silica content up to a weight fraction of 15%. Maximum proton conductivity at room temperature of 0.034 S cm^{-1} was achieved for

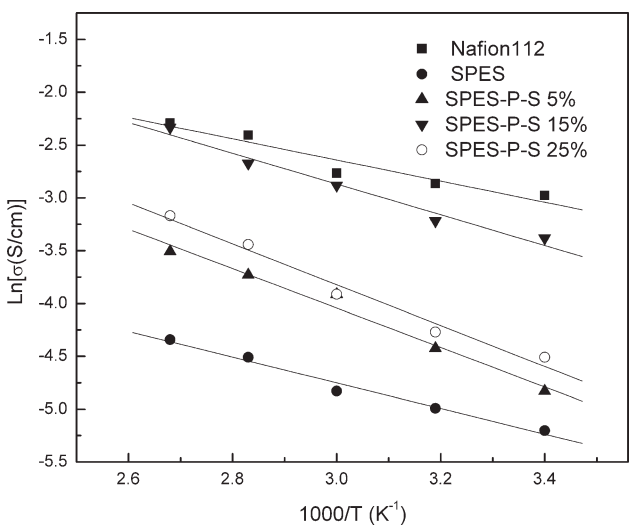

Figure 9 Influence of temperature on proton conductivity of Nafion 112 and SPES-P-S composite membranes.

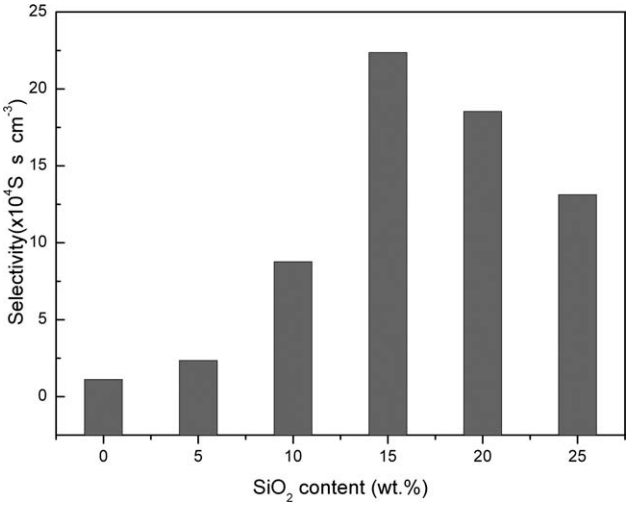

Figure 10 The selectivity of composite membranes.

the SPES-P-S 15% composite membrane. This behavior can presumably be attributed to the following two factors: (1) the silica network that was incorporated in composite membranes by a sol-gel method absorbed many water molecules. This water-rich surrounding enabled the PWA to be an effective proton conductor; (2) the enhanced acidity of the sulfonic acid in the polymer matrix caused by PWA incorporation.[22] However, the continuous slightly decrease in proton conductivity above 15% silica loading may result from the nonconductive of hygroscopic oxides themselves and the loss of ionic sites (SO_3^-). The loss of ionic sites is presumably because of the strong hydrogen bonding interaction between the sulfonic acid and the PWA molecules.

Methanol permeability

In DMFCs, the proton exchange membranes with low methanol permeability values are required because methanol diffusion from the anode to the cathode leads to lower cell voltage and fuel efficiency. The methanol permeability values of the composite membranes and Nafion 112 membrane at room temperature were measured, and the results were listed in Table II. The value of methanol permeability for Nafion 112 membrane was 1.05×10^{-6} $cm^2\ s^{-1}$, which was closed to the value measured by Jang.[25] Compared with Nafion 112 membrane, all the SPES-P-S composite membranes including the pure SPES membrane had lower methanol permeability. Furthermore, the value of methanol permeability decreased with the increase of silica and PWA content. The reason is possibly as follows: the hydrophilic silica particles, which formed by the hydrolyzation and condensation catalyzed by PWA, may mainly exist around the hydrophilic ion-cluster (or ion channels) and will change the microstructure of SPES, increasing the tortuosity of the methanol transport channels.

As one crucial part of the DMFCs, the electrolyte membranes must have both excellent proton conductivity and low methanol permeation. To compare the comprehensive character of the membranes, a new parameter, selectivity (S), the ratio of proton conductivity to methanol permeability, was defined. The higher S value, the better the membrane performance[24]. The S values of membranes investigated in this work are compared in Figure 10. When the silica loading was below 15 wt % in the composite membranes, the selectivity increased with increasing silica content. The SPES-P-S 15% membrane had the highest selectivity in our experiments, 2.24×10^5 S s cm^{-3}, which is almost five times than that of Nafion 112 membrane. The SPES-P-S composite membranes can therefore be a viable substitute for Nafion in DMFCs.

CONCLUSIONS

The SPES/PWA/SiO_2 composite membranes with various PWA and silica loadings were prepared by doping SiO_2 sol and PWA in the SPES matrix. The effect of PWA and silica on the properties of composite membranes was evaluated by thermal stability, water uptake, morphology, proton conductivity, and methanol permeability. The composite membranes showed higher thermal stability and T_g than the pure SPES membrane. Water uptake of the membranes was enhanced by incorporating of PWA and silica into SPES matrix. The SPES-P-S 15% composite membrane showed highest proton conductivity (0.034 S cm^{-1}), which was similar to that of Nafion 112 membrane. And especially, the methanol permeability of the composite membranes was very excellent. The excellent comprehensive property of the composite membrane suggests their suitability as electrolytes in DMFCs applications.

The authors are grateful to BASF for kindly providing PES materials.

References

1. Lee, C.; Sundar, S.; Kwon, J.; Han, H. J Polym Sci Part A: Polym Chem 2004, 42, 3612.
2. Hasani-Sadrabadi, M. M.; Ghaffarian, S. R.; Mokarram-Dorri, N.; Dashtimoghadam, E.; Majedi, F. S. Solid State Ionics 2009, 180, 1497.
3. Li, X.; Liu, C.; Xua, D.; Zhao, C.; Wang, Z.; Zhang, G.; Na, H.; Xing, W. J Power Sources 2006, 162, 1.
4. Rhee, C. H.; Kim, H. K.; Chang, H.; Lee, J. S. Chem Mater 2005, 17, 1691.
5. Shu, Y. C.; Chuang, F. S.; Tsen, W. C.; Chow, J. D.; Gong, C.; Wen, S. J Appl Polym Sci 2008, 108, 1783.
6. Jiang, R.; Kunz, H. R.; Fenton, J. M. J Membr Sci 2006, 272, 116.
7. Mauritz, K. A.; Payne, J. T. J Membr Sci 2000, 168, 39.

8. Tsai, J. C.; Kuo, J. F.; Chen, C. Y. J Power Sources 2007, 174, 103.
9. Lee, C. H.; Mina, K. A.; Park, H. B.; Hong, Y. T.; Jung, B. O.; Lee, Y. M. J Membr Sci 2007, 303, 258.
10. Wen, S.; Gong, C.; Tsen, W. C.; Shu, Y. C.; Tsai, F. C. Int J Hydrogen Energy 2009, 34, 8982.
11. Wen, S.; Gong, C.; Tsen, W. C.; Shu, Y. C.; Tsai, F. C. J Appl Polym Sci 2010, 116, 1491.
12. Wang, Z.; Ni, H.; Zhao, C.; Li, X.; Fu, T.; Na, H. J Polym Sci Part A-2: Polym Phys 1967 2006, 44.
13. Zhang, H.; Zhu, B.; Xu, Y. Solid State Ionics 2006, 177, 1123.
14. Ramani, V.; Kunz, H. R.; Fenton, J. M. J Membr Sci 2004, 232, 31.
15. Staiti, P.; Aricò, A. S.; Baglio, V.; Lufrano, F.; Passalacqua, E.; Antonucci, V. Solid State Ionics 2001, 145, 101.
16. Shao, Z.; Joghee, P.; Hsing, I. J Membr Sci 2004, 229, 43.
17. Kim, Y. S.; Wang, F.; Hickner, M.; Zawodzinski, T. A.; McGrath, J. E. J Membr Sci 2003, 212, 263.
18. Dai, H.; Guan, R.; Li, C.; Liu, J. Solid State Ionics 2007, 178, 339.
19. Cui, W.; Kerres, J.; Eigenberger, G. Sep Purification Technol 1998, 14, 145.
20. Swier, S.; Shaw, M. T.; Weiss, R. A. J Membr Sci 2006, 270, 22.
21. Guan, R.; Dai, H.; Li, C.; Liu, J.; Xu, J. J Membr Sci 2006, 277, 148.
22. Choi, J. K.; Lee, D. K.; Kim, Y. W.; Min, B. R.; Kim, J. H. J Polym Sci Part B: Polym Phys 2008, 46, 691.
23. Xu, W.; Lu, T.; Liu, C.; Xing, W. Electrochim Acta 2005, 50, 3280.
24. Shen, Y.; Qiu, X.; Shen, J.; Xi, J.; Zhu, W. J Power Sources 2006, 161, 54.
25. Jang, W.; Sundar, S.; Choi, S.; Shul, Y. G.; Han, H. J Membr Sci 2006, 280, 321.